Journal of Applied Analysis and Computation
Volume 11, Number 5, October 2021, 2611–2629
Website:http://www.jaac-online.com
DOI:10.11948/20210102

A DYNAMIC MODEL FOR COVID-19 THERAPY WITH DEFECTIVE INTERFERING PARTICLES AND ARTIFICIAL ANTIBODIES*

Yanfei Zhao[1] and Yepeng Xing[1,†]

Abstract In this paper, we use ordinary differential equations to propose a mathematical model for COVID-19 therapy with both defective interfering particles and artificial antibodies. For this model, the basic reproduction number $\mathcal{R}_0$ is given and its threshold properties are discussed. We investigate the global asymptotic stability of disease-free equilibrium E_0 and infection equilibrium without defective interfering particles E_1 by utilizing Lyapunov function and LaSalle's invariance principle. For infection equilibrium with defective interfering particles E_2, stability and Hopf bifurcation results are presented. Numerical simulation is also given to demonstrate the applicability of the theoretical predictions.

Keywords COVID-19 dynamic model, basic reproductive number, Lyapunov function, LaSalle invariance principle

MSC(2010) 34C60, 92B05.

1. Introduction

The global epidemic of coronavirus disease 2019 (COVID-19) is now a major global health threat. COVID-19 is the result of infection with severe acute respiratory syndrome coronavirus 2(SARS-CoV-2) that is an enveloped positive-sense single-stranded RNA virus belongs to coronavirus (CoV) family [22]. This is the third zoonotic human coronavirus emerging in the current century, after the severe acute respiratory syndrome coronavirus (SARS-CoV) in 2002 that spread to 37 countries and the Middle East respiratory syndrome coronavirus (MERS-CoV) in 2012 that spread to 27 countries [6].

Typical symptoms of COVID-19 infection include dry cough, fever, fatigue, breathing difficulty, and bilateral lung infiltration in severe cases [11]. Older people, and those with underlying medical problems like cardiovascular disease, diabetes, chronic respiratory disease, and cancer are more likely to develop serious illness [6]. Respiratory droplet and contact transmission are the main transmission routes for person-to-person spread of SARS-CoV-2. Other potential routes include aerosol and fecal-oral transmissions, which have not yet been confirmed [17]. Thus, current works are focused on containment and quarantine of infected individuals, while researchers are trying them best to find methods to analyze the

†The corresponding author. Email: ypxing@shnu.edu.cn(Y. Xing)
[1]Department of Mathematics, Shanghai Normal University, Road Guilin N0.100, 200234, Shanghai, China
*The authors were supported by National Natural Science Foundation of China (No. 12071297).

structure of the virus protein and the viral phylodynamics to produce vaccine [1,16]. Now some vaccines are approved but not available for every country for disease prevention and treatment [14]. An effective therapy is still important for the patients infected with COVID-19 today. Some experts are making great efforts in seeking specific medicine which treats this disease. The main method is to inhibit the replication and infection of the virus. Defective interfering particles(DIPs) and artificial antibodies offer alternative approaches.

The therapy for COVID-19 uses defective interfering particles to prevent the replication of virus was proposed by Spanish reaschers. Defective interfering particles (DIPs) lack an essential portion of the virus genome, but retain signals for replication and packaging, and therefore, interfere with standard virus (STV) replication [4, 7, 21]. Influenza A virus (IAV) defective interfering particles (DIPs) were previously proposed for antiviral treatment against Influenza A infections [18,20,25]. In the nearest study, it conducted in vitro co-infection experiments with produced, cell culture-derived DIPs and the IFN-sensitive SARS-CoV-2. It showed that treatment with IAV DIPs leads to complete abrogation of SARS-CoV-2 replication [15]. This study provides evidence that defective interefering particles(DIPs) could similarly inhibit SARS-CoV-2 in patients. The therapy for COVID-19 uses artificial antibodies to neutralize virus was introduced in [9]. The coronavirus binds to angiotensin-converting enzyme 2 (ACE2) through its S protein on the virion, and then the viral membrane fuses with the cell membrane. Subsequently, the RNA virus will replicate its genome inside the cell, and ultimately make new virions that will be secreted to infect other cells [12, 19]. Artificial antibodies were proposed to bind to the S protein of 2019-nCoV thereby neutralizing the virus(Figure 1) [9]. LY-CoV555 (also known as LY3819253), a potent antispike neutralizing monoclonal antibody was developed by Eli Lilly after its discovery by researchers at AbCellera and at the Vaccine Research Center of the National Institute of Allergy and Infectious Diseases. A research showed that artificial antibody LY-CoV555 appeared to accelerate the natural decline in viral load over time [3].

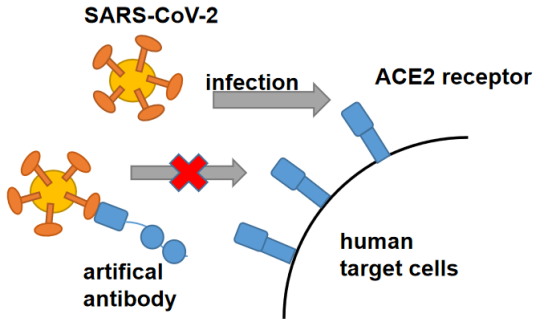

Figure 1. Artificial antibodies block SARS-CoV-2 from infecting cells.

In this paper, we consider to combine the above two potential treatments and we propose a mathematical model to understand this approach of fighting a virus with DIPs and artificial antibodies. Mathematical models can provide insights into the dynamics of viral load in vivo. We use the model to determine the role of the DIPs and artificial antibodies. The paper is structured as follows. In section 2, we formulate a mathematical model of COVID-19 describing the effects of defective

interfering particles(DIPs) and artificial antibodies. In section 3, we will discuss the well-posedness of the solutions, equilibria and their stability. Also, in order to properly define biologically meaningful equilibria, the basic reproduction number $\mathcal{R}_0$ will be defined. we analyze the stability of the three equilibria: disease-free equilibrium E_0, infection equilibrium without defective interfering particles E_1, and infection equilibrium with defective interfering particles E_2. It will be shown that E_0 is globally asymptotically stable for $0 < \mathcal{R}_0 < 1$, E_1 is globally asymptotically stable for $\mathcal{R}_0 > 1, R_1 < 1$, where R_1 is a constant defined in terms of the system parameters, and E_2 is asymptotically stable for $R_1 < \mathcal{R}_0 < R_2$, where R_2 denotes a Hopf critical point from which a family of limit cycles bifurcate. A numerical example is present in Section 4 to demonstrate the theoretical predictions. Finally, conclusion and discussion are drawn in Section 5.

2. Model formulation

A standard and classic virus dynamical model is the following system of ordinary differential equations (ODEs) [2, 13]:

$$\begin{aligned} \frac{dx}{dt} &= \lambda - dx - \beta xv, \\ \frac{dy}{dt} &= \beta xv - ay, \\ \frac{dv}{dt} &= ky - pv, \end{aligned} \tag{2.1}$$

where $x(t)$, $y(t)$ and $v(t)$ are the densities of uninfected target cells, infected target cells and the free virus, respectively, at time t. The infection rate is β. The healthy cell is assumed to be produced at a constant rate λ. It is also assumed that once cells are infected, they may die at rate a, either due to the action of the virus or the immune system, and in the mean time, they each produces virus particles at a rate k during their life which on average has length $1/a$.

In this paper, let $T(t)$ is the density of susceptible host cells, $I(t)$ is the density of infected cells, $V(t)$ is the density of free virus, $W(t)$ is the density of defective interfering particles, and $F(t)$ is the density of artificial antibodies. Normal cells are produced at a constant rate λ, and die at a rate d_1T. The infection rate is equal to αTV, and infected cells die at a rate d_2I. The virus are removed from the plasma at a rate d_3V and the antibody as enhancement of viral clearance at a rate η_2FV. The defective interfering particle attacks infected cells at a rate η_1WI and the inhibition function of the virus at a rate $1+\beta W$. The infected cells relasing defective interfering particles at a rate $k\eta_1WI$. And so with the pressure of interfering particles the virus production rate is given by $\gamma I/(1 + \beta W)$. The death rate of defective interfering particle is d_4W. d_5F is the death rate of artificial antibody(Figure 2). The system describing these interactions is given by

$$\begin{aligned} \frac{dT}{dt} &= \lambda - \alpha TV - d_1T, \\ \frac{dI}{dt} &= \alpha TV - d_2I - \eta_1WI, \\ \frac{dV}{dt} &= \frac{\gamma I}{1 + \beta W} - d_3V - \eta_2FV, \end{aligned} \tag{2.2}$$

$$\frac{dW}{dt} = k\eta_1 WI - d_4 W,$$
$$\frac{dF}{dt} = -\eta_2 FV - d_5 F.$$

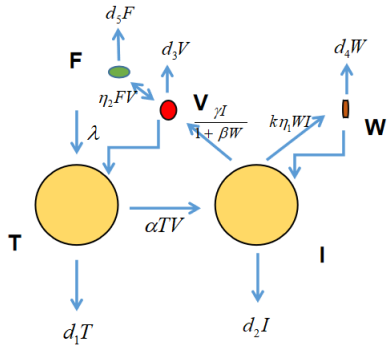

Figure 2. Pathogen viral particles V infect normal cells T, producing infected cells I; W can infect infected cells, artificial antibodies F bind to virus, infected cells are able to produce virus V and defective interfering particles W.

3. Analytical results

3.1. Positivity and boundedness of solutions

First, we assume that the initial conditions for the system (2.2) have the form

$$T(0) = T_0 > 0, \quad I(0) = I_0 > 0, \quad V(0) = V_0 > 0,$$
$$W(0) = W_0 > 0, \quad F(0) = F_0 > 0. \tag{3.1}$$

Since the right hand side functions of (2.2) satisfy the Lipschitz condition, there is a unique solution with the initial conditions (3.1). Because of biological reasons, all variables in system (2.2) must be non-negative. Therefore, for non-negative initial values (3.1), the corresponding solution must remain non-negative. This can be confirmed as below.

Theorem 3.1. *The solution of system (2.2) subjects to initial conditions (3.1) is positive for all* $t \geq 0$.

Proof. From the first equation of (2.2), we have

$$T(t) = e^{-\int_0^t (d_1+\alpha V(s))ds} T(0) + \lambda \int_0^t e^{-\int_s^t (d_1+\alpha V(p))dp} ds,$$

implying $T(t) > 0$ for all $t \geq 0$.

Similarly, we can easily prove $W(t) > 0$ for all $t \geq 0$.

Next, we prove that $I(t)$ and $V(t)$ are positive for all $t \geq 0$. We assume that $t_i, i = 1, 2$ are the first times when $I(t)$ and $V(t)$ reach zero, respectively, and $t_0 = \min\{t_1, t_2\}$. We discuss the following three cases.

If $t_0 = t_1$, then

$$\begin{aligned} &I(t) > 0, \quad V(t) > 0, \qquad t \in [0, t_1), \\ &I(t_1) = 0, \quad V(t_1) > 0, \qquad t = t_1. \end{aligned}$$

From the second equation in (2.2), we observe that

$$\frac{dI(t)}{dt}|_{t=t_1} = \alpha T(t_1)V(t_1) > 0.$$

That means $I(t) < 0$ for $t \in (t_1 - \epsilon, t_1)$, where ϵ is an arbitrarily small positive constant. This is a contradiction.

If $t_0 = t_2$, then

$$\begin{aligned} &V(t) > 0, \quad I(t) > 0, \qquad t \in [0, t_2), \\ &I(t_2) > 0, \quad V(t_2) = 0, \qquad t = t_2. \end{aligned}$$

From the third equation in (2.2), we have

$$\frac{dV(t)}{dt}|_{t=t_2} = \frac{\gamma I(t_2)}{1 + \beta W(t_2)} > 0.$$

That means $V(t) < 0$ for $t \in (t_2 - \epsilon, t_2)$, where ϵ is an arbitrarily small positive constant. This is a contradiction.

If $t_0 = t_1 = t_2$, from the second equation in (2.2), we have

$$I(t) = e^{-\int_0^t (d_2 + \eta_1 W(s))ds} I(0) + \int_0^t \alpha T(s)V(s)e^{-\int_s^{t_0} (d_2 + \eta_1 W(p))dp})ds. \tag{3.2}$$

Letting $t = t_0$ in (3.2), we have

$$\begin{aligned} I(t_0) &= e^{-\int_0^{t_0} (d_2 + \eta_1 W(s))ds} I(0) + \int_0^{t_0} \alpha T(s)V(s)e^{-\int_s^{t_0} (d_2 + \eta_1 W(p))dp})ds \\ &> e^{-\int_0^{t_0} (d_2 + \eta_1 W(s))ds} I(0) > 0, \end{aligned}$$

which is in contradiction to $I(t_0) = 0$.

Finally, we can prove $F(t) > 0$ for all $t \geq 0$. From the fifth equation of (2.2), we can get

$$F(t) = e^{-\int_0^t (d_5 + \eta_2 V(s))ds} F(0),$$

implying $F(t) > 0$ for all $t \geq 0$. □

Theorem 3.2. *The solution of system (2.2) subjects to initial conditions (3.1) is bounded for all $t \geq 0$.*

Proof. Let $\Lambda(t) = T(t) + I(t) + \frac{d_2}{2\gamma} V(t) + \frac{1}{k} W(t) + F(t)$ and $\mu = \min \left\{ d_1, \frac{d_2}{2}, \frac{d_2 d_3}{2\gamma}, \frac{d_4}{k}, d_5 \right\}$. By straightforward computation, we have

$$\frac{d\Lambda(t)}{dt} \leq \lambda - \mu\Lambda(t),$$

which implies that

$$\Lambda(t) \leq \max\left\{\Lambda(0), \frac{\lambda}{\mu}\right\}.$$

Since the solution of system (2.2) subjects to initial conditions is positive for all $t \geq 0$. This implies that $\Lambda(t)$ is bounded, so are $T(t), I(t), V(t), W(t)$ and $F(t)$. □

3.2. Equilibria and basic reproduction number

System (2.2) has three possible biologically meaningful equilibria: disease-free equilibrium E_0, infection equilibrium without defective interfering particles E_1, infection equilibrium with defective interfering particles E_2, given as follows:

$$\begin{aligned} E_0 &= (\frac{\lambda}{d_1}, 0, 0, 0, 0), \\ E_1 &= (\frac{d_2 d_3}{\alpha\gamma}, \frac{\lambda}{d_2}(1 - \frac{1}{\mathcal{R}_0}), \frac{d_1}{\alpha}(\mathcal{R}_0 - 1), 0, 0), \\ E_2 &= (\frac{\lambda R_1}{d_1 \mathcal{R}_0}, \frac{d_4}{k\eta_1}, \frac{d_1}{\alpha}(\frac{\mathcal{R}_0}{R_1} - 1), \frac{d_2}{\eta_1}(R_1 - 1), 0), \end{aligned} \tag{3.3}$$

where $\mathcal{R}_0$ is called the basic reproduction number, defined by

$$\mathcal{R}_0 = \frac{\lambda\alpha\gamma}{d_1 d_2 d_3(1 + \beta w_0)},$$

where w_0 is the number of the defective interfering particles. When there are no defective interfering particles in the humoral environment, w_0 equals to zero.

$$\mathcal{R}_1 = \frac{\lambda\alpha\gamma k\eta_1}{d_2 d_4 \alpha\gamma + k\eta_1 d_1 d_2 d_3(1 + \beta w_0)} = \frac{1}{\frac{d_2 d_4}{\lambda k\eta_1} + \frac{1}{\mathcal{R}_0}}.$$

It can be seen from the expressions of the equilibrium solutions that the disease-free equilibrium E_0, always exists for any values of parameters. The infection equilibrium without defective interfering particles E_1, exists if and only if $\mathcal{R}_0 > 0$, while the infection equilibrium with defective interfering particles E_2, exists if and only if $\mathcal{R}_0 > R_1 > 1$. In order to analyze the local stability of system (2.2) at an equilibrium E, we need to calculate the Jacobian matrix of system (2.2) at $E = (T, I, V, W, F)$ as below:

$$J(E) = \begin{bmatrix} -\alpha V - d_1 & 0 & -\alpha T & 0 & 0 \\ \alpha V & -d_2 - \eta_1 W & \alpha T & -\eta_1 I & 0 \\ 0 & \frac{\gamma}{1 + \beta W} & -d_3 - \eta_2 F & \frac{-\beta\gamma I}{(1 + \beta W)^2} & -\eta_2 V \\ 0 & k\eta_1 W & 0 & k\eta_1 I - d_4 & 0 \\ 0 & 0 & -\eta_2 F & 0 & -\eta_2 V - d_5 \end{bmatrix}. \tag{3.4}$$

The characteristic equation of system (2.2) at E is $det(\xi I - J) = 0$, whose roots determine the local stability of E.

3.3. Stability of the disease-free equilibrium E_0

First, for the local stability of E_0, we have the following theorem.

Theorem 3.3. *When $\mathcal{R}_0 < 1$, the disease-free equilibrium E_0 is locally asymptotically stable; when $\mathcal{R}_0 > 1$, E_0 becomes unstable.*

Proof. For the disease-free equilibrium E_0, some fundamental calculations give the corresponding characteristic equation

$$(\xi + d_1)(\xi + d_4)(\xi + d_5)(\xi^2 + c_1\xi + c_0) = 0, \tag{3.5}$$

where

$$\begin{aligned} c_1 &= d_2 + d_3, \\ c_0 &= d_2 d_3 - \frac{\lambda\alpha\gamma}{d_1}. \end{aligned}$$

The stability of E_0 by the sign of real parts of the roots of Equation (3.5): If all roots of Equation (3.5) have negative real parts, then E_0 is locally asymptotically stable; if there is at least one root of Equation (3.5) has positive real part, then E_0 is unstable. Obviously, we only should consider the following equation:

$$D(\xi) = \xi^2 + (d_2 + d_3)\xi + d_2 d_3 - \frac{\lambda\alpha\gamma}{d_1} = 0. \tag{3.6}$$

If $\mathcal{R}_0 > 1$, it is easy to show for real ξ that

$$D(0) = d_2 d_3(1 - \mathcal{R}_0) < 0, \quad \lim_{\xi \to +\infty} D(\xi) = +\infty.$$

Hence, D(ξ)=0 has at least one positive real root. Therefore, if $\mathcal{R}_0 > 1$, the disease-free equilibrium E_0 is unstable.

Next, consider $\mathcal{R}_0 < 1$. Using the Decarte's rule of sign, we know that the negativity of the real parts of the two roots of Equation (3.6) is equivalent to $d_2 d_3 - \dfrac{\lambda\alpha\gamma_1}{d_1} > 0$, that is $\mathcal{R}_0 < 1$. Therefore, all roots of (3.6) have negative real part when $\mathcal{R}_0 < 1$, the disease-free equilibrium E_0 is locally asymptotically stable. □

Further, for the global stability of E_0, we have the following result.

Theorem 3.4. *When $\mathcal{R}_0 < 1$, the disease-free equilibrium E_0 is globally asymptotically stable.*

Proof. We consturt the following Lyapunov function:

$$L_1 = \frac{1}{2}(T - \frac{\lambda}{d_1})^2 + \frac{\lambda}{d_1}I + \frac{\lambda d_2}{\gamma d_1}V + \frac{\lambda}{k d_1}W + F. \tag{3.7}$$

Thus, we have

$$\begin{aligned} L_1' &= (T - \frac{\lambda}{d_1})T' + \frac{\lambda}{d_1}I' + \frac{\lambda d_2}{\gamma d_1}V' + \frac{\lambda}{d_1 k}W' + F' \\ &= (T - \frac{\lambda}{d_1})(\lambda - \alpha TV - d_1 T) + \frac{\lambda}{d_1}(\alpha TV - d_2 I - \eta_1 WI) + \frac{\lambda d_2}{\gamma d_1}(\frac{\gamma I}{1 + \beta W} - d_3 V \end{aligned}$$

$$
\begin{aligned}
&- \eta_2 FV) + \frac{\lambda}{d_1 k}(k\eta_1 WI - d_4 W) - (\eta_2 FV + d_5 F) \\
&= (T - \frac{\lambda}{d_1})[-d_1(T - \frac{\lambda}{d_1}) - \alpha TV] + \frac{\lambda}{d_1}\alpha TV + \frac{\lambda}{d_1}(\frac{d_2}{1+\beta W} - d_2)I \\
&\quad - \frac{\lambda d_2(d_3 + \eta_2 F)}{d_1 \gamma} V - \frac{\lambda d_4}{k d_1} W - (\eta_2 FV + d_5 F) \\
&= -d_1(T - \frac{\lambda}{d_1})^2 - (T - \frac{\lambda}{d_1})[\alpha V(T - \frac{\lambda}{d_1}) + \frac{\lambda}{d_1}\alpha V] + \frac{\lambda}{d_1}\alpha V(T - \frac{\lambda}{d_1}) + \frac{\lambda^2 \alpha}{d_1^2} V \\
&\quad + \frac{\lambda}{d_1}(\frac{d_2}{1+\beta W} - d_2)I - \frac{\lambda d_2(d_3 + \eta_2 F)}{d_1 \gamma} V - \frac{\lambda d_4}{k d_1} W - (\eta_2 FV + d_5 F) \\
&= -d_1(T - \frac{\lambda}{d_1})^2 - \alpha V(T - \frac{\lambda}{d_1})^2 + \frac{\lambda d_2 d_3}{\gamma d_1}(\mathcal{R}_0 - 1)V + \frac{\lambda}{d_1}(\frac{d_2}{1+\beta W} - d_2)I \\
&\quad - \frac{\lambda d_2 \eta_2}{d_1 \gamma} FV - \frac{\lambda d_4}{k d_1} W - (\eta_2 FV + d_5 F) \\
&\leq 0. \qquad (3.8)
\end{aligned}
$$

Note that T, I, V, W, F are positive. All terms of the right in (3.8) are non-positive when $\mathcal{R}_0 < 1$. $L_1' = 0$ if and only if $T = \lambda/d_1$ and other variables are zero. By LaSalle's invariance principle [10], we conclude that E_0 is indeed globally asymptotically stable. □

3.4. Stability of the infection equilibrium E_1

When $\mathcal{R}_0 > 1$, the disease-free equilibrium E_0 becomes unstable and bifurcates into the infection equilibrium without defective interfering particles E_1. Thus, in order to study the stability of E_1, we assume $\mathcal{R}_0 > 1$ in this section. We have the following results.

Theorem 3.5. *When $R_1 < 1 < \mathcal{R}_0$, the infection equilibrium without defective interfering particles E_1 is locally asymptotically stable; when $R_1 > 1$, E_1 becomes unstable.*

Proof. The characteristic equation at E_1 is given by

$$
[\xi + \frac{\eta_2 d_1}{\alpha}(\mathcal{R}_0 - 1) + d_5][\xi - \frac{k\eta_1 \lambda}{d_1}(1 - \frac{1}{R_1})](\xi^3 + a_2\xi^2 + a_1\xi + a_0) = 0, \qquad (3.9)
$$

where

$$
\begin{aligned}
a_2 &= d_1 \frac{\mathcal{R}_0}{R_1} + d_2 + d_3, \\
a_1 &= d_1(d_2 + d_3)\frac{\mathcal{R}_0}{R_1}, \\
a_0 &= d_1 d_2 d_3(\mathcal{R}_0 - 1).
\end{aligned}
$$

See that

$$
\xi_1 = \frac{\eta_2 d_1}{\alpha}(1 - \mathcal{R}_0) - d_5 < 0, \quad \xi_2 = \frac{k\eta_1 \lambda}{d_1}(1 - \frac{1}{R_1}) < 0.
$$

Next, we consider the following equation:

$$
\xi^3 + (d_1 \frac{\mathcal{R}_0}{R_1} + d_2 + d_3)\xi^2 + d_1(d_2 + d_3)\frac{\mathcal{R}_0}{R_1}\xi + d_1 d_2 d_3(\mathcal{R}_0 - 1) = 0. \qquad (3.10)
$$

Applying the Routh-Hurwitz Criterion [5], we can get that all roots of (3.10) have negative real parts if and only if $a_2 > 0$, $a_0 > 0$ and $a_1a_2 - a_0 > 0$. Note that

$$\begin{aligned}
&a_2 = d_1\frac{\mathcal{R}_0}{R_1} + d_2 + d_3 > 0,\\
&a_0 = d_1d_2d_3(\mathcal{R}_0 - 1) > 0,\\
&a_1a_2 - a_0 = [d_1(d_2+d_3)\frac{\mathcal{R}_0}{R_1}](d_1\frac{\mathcal{R}_0}{R_1} + d_2 + d_3) - d_1d_2d_3(\mathcal{R}_0 - 1) > 0.
\end{aligned} \tag{3.11}$$

Hence, all roots of the characteristic equation (3.9) have negative real parts. It means that when $R_1 < 1 < \mathcal{R}_0$, the infection equilibrium without defective interfering particles E_1 is locally asymptotically stable. □

Also, we can prove the global stability of E_1, as given in the following theorem.

Theorem 3.6. *When $R_1 < 1 < \mathcal{R}_0$, the infection equilibrium without defective interfering particles E_1 is globally asymptotically stable.*

Proof. For convenience, we denote E_1 as $(T_1, I_1, V_1, 0, 0)$, where $T_1 = \frac{d_2d_3}{\alpha\gamma}$, $I_1 = \frac{\lambda}{d_1}(1 - \frac{1}{\mathcal{R}_0})$ and $V_1 = \frac{d_1}{\alpha}(\mathcal{R}_0 - 1)$. We construst the following Lyapunov function:

$$\begin{aligned}
L_2 =& T - T_1 - T_1\ln\frac{T}{T_1} + I - I_1 - I_1\ln\frac{I}{I_1} + \frac{d_2}{\gamma}(V - V_1 - V_1\ln\frac{V}{V_1})\\
&+ \frac{1}{k}W + \frac{d_2\eta_2}{d_5\gamma}(\frac{\lambda\gamma}{d_2d_3} - \frac{d_1}{\alpha})F.
\end{aligned} \tag{3.12}$$

Thus, we have

$$\begin{aligned}
L_2{}' &= T' - \frac{T_1}{T}T' + I' - \frac{I_1}{I}I' + \frac{d_2}{\gamma}(V' - \frac{V_1}{V}V') + \frac{1}{k}W' + \frac{d_2\eta_2}{d_5\gamma}(\frac{\lambda\gamma}{d_2d_3} - \frac{d_1}{\alpha})F'\\
&= d_1T_1(2 - \frac{T}{T_1} - \frac{T_1}{T}) + \alpha T_1V + \alpha T_1V_1 - \frac{\alpha T_1^2V_1}{T} + (\frac{d_2}{1+\beta W} - d_2)I\\
&\quad - \frac{I_1}{I}\alpha TV + d_2I_1 + (\eta_1I_1 - \frac{d_4}{k})W - (\frac{d_2d_3}{\gamma} + \frac{d_2\eta_2}{\gamma}F)V - \frac{V_1}{V}\frac{d_2I}{1+\beta W}\\
&\quad + \frac{d_2d_3}{\gamma}V_1 - \frac{d_2\eta_2^2}{d_5\gamma}FV\\
&= d_1T_1(2 - \frac{T}{T_1} - \frac{T_1}{T}) + \alpha T_1V + \alpha T_1V_1 - \frac{\alpha T_1^2V_1}{T} + (\frac{d_2}{1+\beta W} - d_2)I\\
&\quad - \frac{I_1}{I}\alpha TV + \alpha T_1V_1 + (\eta_1I_1 - \frac{d_4}{k})W - (\frac{d_2d_3}{\gamma} + \frac{d_2\eta_2}{\gamma}F)V - \frac{V_1}{V}\frac{d_2I}{1+\beta W}\\
&\quad + \alpha T_1V_1 - \frac{d_2\eta_2^2}{d_5\gamma}FV\\
&= d_1T_1(2 - \frac{T}{T_1} - \frac{T_1}{T}) + 3\alpha T_1V_1 + \alpha T_1V - \frac{\alpha T_1^2V_1}{T} - \frac{I_1}{I}\alpha TV - \frac{V_1}{V}\frac{d_2I}{1+\beta W}\\
&\quad + (\frac{d_2}{1+\beta W} - d_2)I + (\eta_1I_1 - \frac{d_4}{k})W - \frac{d_2}{\gamma}(d_3 + \eta_2F)V - \frac{d_2\eta_2^2}{d_5\gamma}FV\\
&\le d_1T_1(2 - \frac{T}{T_1} - \frac{T_1}{T}) + \alpha T_1V_1(3 - \frac{T_1}{T} - \frac{TVI_1}{T_1V_1I} - \frac{d_2I}{VT_1}) + (\frac{d_2}{1+\beta W} - d_2)I
\end{aligned}$$

$$
\begin{aligned}
&+(\eta_1 I_1-\frac{d_4}{k})W-\frac{d_2}{\gamma}(d_3+\eta_2 F)V-\frac{d_2\eta_2^2}{d_5\gamma}FV\\
&\le d_1T_1(2-\frac{T}{T_1}-\frac{T_1}{T})+3\alpha T_1V_1(1-\sqrt[3]{\frac{T_1}{T}\frac{TVI_1}{T_1V_1I}\frac{d_2I}{VT_1}})+(\frac{d_2}{1+\beta W}-d_2)I\\
&+(\eta_1 I_1-\frac{d_4}{k})W-\frac{d_2}{\gamma}(d_3+\eta_2 F)V-\frac{d_2\eta_2^2}{d_5\gamma}FV\\
&=d_1T_1(2-\frac{T}{T_1}-\frac{T_1}{T})+3\alpha T_1V_1(1-\sqrt[3]{\frac{d_2I_1}{\alpha T_1V_1}})+(\frac{d_2}{1+\beta W}-d_2)I\\
&+\frac{\lambda\eta_1 k}{d_1}(1-\frac{1}{R_1})W-\frac{d_2}{\gamma}(d_3+\eta_2 F)V-\frac{d_2\eta_2^2}{d_5\gamma}FV. \qquad (3.13)
\end{aligned}
$$

Clearly, $L_2{}' \le 0$ since $\mathcal{R}_1 < 1$. $L_2{}' = 0$ if and only if $(T, I, V, W, F) = E_1$. By LaSalle's invariance principle [10], we conclude that E_1 is globally asymptotically stable. □

3.5. Stability of the infection equilibrium E_2

When $R_1 > 1$, the infection equilibrium without defective interfering particles E_1 becomes unstable and there appears another infection equilibrium with defective interfering particles E_2. To discuss the stability of E_2, we assume $\mathcal{R}_0 > R_1$ in this section. In order to simplify the analysis for the equilibrium E_2, we first take the following scalings to reduce the number of parameters:

$$
\begin{aligned}
&T\to\mu_1 T,\quad I\to\mu_2 I,\quad V\to\mu_3 V,\quad W\to\mu_4 W,\quad F\to\mu_5 F,\quad \tau=\phi t,\\
&\frac{d_1}{\phi}\to d_1,\quad \frac{d_2}{\phi}\to d_2,\quad \frac{d_3}{\phi}\to d_3,\quad \frac{d_4}{\phi}\to d_4,\quad \frac{d_5}{\phi}\to d_5,\quad \frac{\eta_1}{\beta\phi}\to\eta_1,\\
&\frac{\alpha\gamma}{k\eta_1\phi}\to\gamma,\quad \frac{\eta_2}{\alpha}\to\eta_2,
\end{aligned} \qquad (3.14)
$$

where

$$
\phi=\sqrt{\lambda k\eta_1},\quad \mu_1=\mu_2=\frac{\phi}{k\eta_1},\quad \mu_3=\frac{\phi}{\alpha},\quad \mu_4=\frac{1}{\beta},\quad \mu_5=\frac{\phi}{\eta_2}. \qquad (3.15)
$$

Then, system (2.2) is transformed into

$$
\begin{aligned}
\frac{dT}{d\tau}&=1-TV-d_1T,\\
\frac{dI}{d\tau}&=TV-d_2I-\eta_1WI,\\
\frac{dV}{d\tau}&=\frac{\gamma I}{1+W}-d_3V-FV,\\
\frac{dW}{d\tau}&=WI-d_4W,\\
\frac{dF}{d\tau}&=-\eta_2FV-d_5F.
\end{aligned} \qquad (3.16)
$$

Now for system (3.16), equilibrium solution E_2, $\mathcal{R}_0$ and R_1 are given as follows:

$$
E_2=(T_2,I_2,V_2,W_2,F_2)=(\frac{R_1}{d_1\mathcal{R}_0},d_4,d_1(\frac{\mathcal{R}_0}{R_1}-1),\frac{d_2}{\eta_1}(R_1-1),0),
$$

$$\mathcal{R}_0 = \frac{\gamma}{d_1 d_2 d_3 (1+w_0)}, \quad R_1 = \frac{\gamma}{d_1 d_2 d_3 (1+w_0) + d_2 d_4 \gamma}, \tag{3.17}$$

where

$$w_0 = \frac{-(1+\frac{\gamma d_4}{d_1 d_3} + \frac{d_2}{\eta_1}) + \sqrt{(1+\frac{\gamma d_4}{d_1 d_3} + \frac{d_2}{\eta_1})^2 + 4(\frac{\gamma}{d_1 d_3 \eta_1} - \frac{d_2 d_4 \gamma}{d_1 d_3 \eta_1} - \frac{d_2}{\eta_1})}}{2}. \tag{3.18}$$

The Jacobian matrix of system (3.16) evaluated at E_2 is

$$J(E) = \begin{bmatrix} -V_2 - d_1 & 0 & -T_2 & 0 & 0 \\ V_2 & -d_2 - \eta_1 W_2 & T_2 & -\eta_1 I_2 & 0 \\ 0 & \frac{\gamma}{1+W_2} & -d_3 - F_2 & \frac{-\gamma I_2}{(1+W_2)^2} & -V_2 \\ 0 & W_2 & 0 & I_2 - d_4 & 0 \\ 0 & 0 & -\eta_2 F_2 & 0 & -\eta_2 V_2 - d_5 \end{bmatrix}. \tag{3.19}$$

For the local stability of E_2, we have the following theorem.

Theorem 3.7. *There exists an R_2 such that when $R_1 < \mathcal{R}_0 < R_2$, the infection equilibrium with defective interefering particles E_2 is locally asymptotically stable.*

Proof. From (3.19), we obtain the corresponding characteristic equation

$$(\xi + d_1 \frac{\mathcal{R}_0}{R_1})(\xi^4 + b_3\xi^3 + b_2\xi^2 + b_1\xi + b_0) = 0, \tag{3.20}$$

where

$$b_3 = d_1 \frac{\mathcal{R}_0}{R_1} + d_2 R_1 + d_3,$$

$$b_2 = d_1 d_2 \mathcal{R}_0 + d_1 d_3 \frac{\mathcal{R}_0}{R_1} + d_2 d_4 (R_1 - 1),$$

$$b_1 = d_1 d_2 d_3 (\mathcal{R}_0 - R_1) + d_2 d_4 (R_1 - 1)(d_3 + d_1 \frac{\mathcal{R}_0}{R_1}) + \frac{d_1 d_2^2 d_3^2}{\eta_1 \gamma} (\mathcal{R}_0 - R_1)(R_1 - 1),$$

$$b_0 = d_1 d_2 d_3 d_4 (\mathcal{R}_0 - \frac{\mathcal{R}_0}{R_1}) + \frac{d_1^2 d_2^2 d_3^2}{\eta_1 \gamma} (R_1 - 1)(\mathcal{R}_0 - R_1).$$

Clearly, it follows from $R_0 > R_1$ that $b_i > 0$ for $i = 0, 1, 2, 3$. Note that (3.21) has a characteristic root $\xi_1 = -d_1 \frac{\mathcal{R}_0}{R_1} < 0$. We next discuss the sign of the other four roots of equation (3.21). Consider the following equation:

$$\xi^4 + b_3\xi^3 + b_2\xi^2 + b_1\xi + b_0 = 0. \tag{3.21}$$

Using Routh-Hurwitz Criterion [5], the necessary and sufficient conditions for the equilibrium E_2 to be asymptotically stable are: $\Delta_i > 0$, $i = 1, 2, 3, 4$, where

$$\Delta_1 = b_3,$$

$$\begin{aligned}\Delta_2 &= b_2b_3 - b_1b_4,\\ \Delta_3 &= b_1\Delta_2 - b_0b_3^2,\\ \Delta_4 &= b_0\Delta_3.\end{aligned} \tag{3.22}$$

It is obviously that $\Delta_1 = b_3 > 0$ and $\Delta_4 = b_0\Delta_3 > 0$ when $\Delta_3 > 0$. Note that

$$\begin{aligned}\Delta_2 &= d_2^2d_4R_1(R_1-1) + d_1d_2d_3R_1 + d_1d_2\mathcal{R}_0(d_1\frac{\mathcal{R}_0}{R_1} + d_2R_1 + d_3)\\ &\quad + d_1d_3\frac{\mathcal{R}_0}{R_1}(d_1\frac{\mathcal{R}_0}{R_1} + d_3) - \frac{d_1d_2^2d_3^2}{\eta_1\gamma}(\mathcal{R}_0 - R_1)(R_1-1),\end{aligned} \tag{3.23}$$

$$\begin{aligned}\Delta_3 &= [d_1d_2d_3(\mathcal{R}_0 - R_1) + d_2d_4(R_1-1)(d_3 + d_1\frac{\mathcal{R}_0}{R_1}) + \frac{d_1d_2^2d_3^2}{\eta_1\gamma}(R_1-1)(\mathcal{R}_0-R_1)]\\ &\quad [d_2^2d_4R_1(R_1-1) + d_1d_2d_3R_1 + d_1d_2\mathcal{R}_0(d_1\frac{\mathcal{R}_0}{R_1} + d_2R_1 + d_3)\\ &\quad + d_1d_3\frac{\mathcal{R}_0}{R_1}(d_1\frac{\mathcal{R}_0}{R_1} + d_3) - \frac{d_1d_2^2d_3^2}{\eta_1\gamma}(\mathcal{R}_0 - R_1)(R_1-1)] - [d_1d_2d_3d_4(\mathcal{R}_0 - \frac{\mathcal{R}_0}{R_1})\\ &\quad + \frac{d_1^2d_2^2d_3^2}{\eta_1\gamma}(R_1-1)(\mathcal{R}_0-R_1)][d_1\frac{\mathcal{R}_0}{R_1} + d_2R_1 + d_3]^2.\end{aligned} \tag{3.24}$$

We cann't determine the signs of Δ_2 and Δ_3 for general $\mathcal{R}_0$. Hence, we take a continuity argument below. We assume $0 < \mathcal{R}_0 - R_1 < \epsilon$, ϵ is an arbitrarily small constant. By straight computation, we get

$$\begin{aligned}\Delta_2 &> d_1^2d_3 + d_1d_3^2 + 2d_1d_2d_3R_1 + d_2^2d_4R_1(R_1-1) + d_1^2d_2R_1 + d_1d_2^2R_1^2\\ &\quad - \epsilon(R_1-1)\frac{d_1d_2^2d_3^2}{\eta_1\gamma},\end{aligned} \tag{3.25}$$

$$\begin{aligned}\Delta_3 &> d_2d_4(R_1-1)[d_1^2d_2d_3\mathcal{R}_1 + d_1d_2^2d_4R_1(R_1-1) + d_1^2d_2R_1(d_1 + d_2R_1)]\\ &\quad - \epsilon^2[\frac{d_1^2d_2^3d_3^3}{\eta_1\gamma}(R_1-1) + \frac{d_1^2d_2^4d_3^4}{{\eta_1}^2\gamma^2}(R_1-1)^2] - \epsilon[d_1d_2^2d_3^2d_4(R_1-1)\mathcal{R}_0\\ &\quad + \frac{d_1d_2^3d_3^2d_4}{\eta_1\gamma}(R_1-1)(d_3 + d_1\frac{\mathcal{R}_0}{R_1})(R_1-1)\\ &\quad + \frac{d_1^2d_2^2d_3^3}{\eta_1\gamma}(R_1-1)(d_1\frac{\mathcal{R}_0}{R_1} + d_2R_1 + d_3)^2].\end{aligned} \tag{3.26}$$

Note that $\Delta_2 > 0$ and $\Delta_3 > 0$ when ϵ is small enough. Then there must exist a $R_2 > 0$ such that both $\Delta_2 > 0$ and $\Delta_3 > 0$ if $R_1 < \mathcal{R}_0 < R_2$. This implies the infection equilibrium E_2 is asymptotically stable by Routh-Hurwitz Criterion. □

When $\mathcal{R}_0$ is increased, Δ_3 and Δ_2 may become negative. The following lemma identifies the order of possible sign switches for Δ_2 and Δ_3.

Lemma 3.1. *If Δ_2 and Δ_3 can change signs from positive to negative as $\mathcal{R}_0$ is increased after the value R_2 in Theorem 3.7, then Δ_3 becomes negative before Δ_2 does.*

Proof. First, we prove that when Δ_2=0, Δ_3 has already been negative.

From (3.22), when $\Delta_2 = 0$,

$$\Delta_3 = -b_0b_3^2 < 0. \tag{3.27}$$

On the other hand, we prove that when $\Delta_3 = 0$, Δ_2 still positive.
From (3.22), when $\Delta_3 = 0$,

$$\Delta_2 = \frac{b_0 b_3^2}{b_1} > 0. \tag{3.28}$$

This completes the proof. □

The above discussion and theorem 2 in Yu [23] imply that Hopf bifurcation can occur when $\Delta_3 = 0$. We have the following result.

Theorem 3.8. *For some large values of d_4 and small values of d_2, there exists a γ_0 satisfying $\mathcal{R}_0 > R_1 > 1$ and $\Delta_3 = 0$, at which the equilibrium E_2 loses its stability through Hopf bifurcation, which gives rise to a family of limit cycles.*

Proof. We have known that $\Delta_3 > 0$ when $0 < \mathcal{R}_0 - R_1 < \epsilon$. In order to show that Hopf bifurcation can occur, we need to show that Δ_3 can change sign from positive to negative as $\mathcal{R}_0$ increases after R_2. Note that

$$\frac{\mathcal{R}_0}{R_1} = \frac{d_4\gamma}{d_1 d_3(1+w_0)} + 1. \tag{3.29}$$

We consider small values of d_2 and large values of d_4. Note that

$$R_1 = \frac{\gamma}{d_1 d_2 d_3(1+w_0) + d_2 d_4 \gamma}.$$

We assume $d_2 d_4 = m < 1$. Without loss of generality, we suppose d_2 is sufficiently small, d_4 is sufficiently large in the following discussion. From (3.22), we can obtain

$$\Delta_3 = \frac{1}{[d_4\gamma + d_1 d_3(1+w_0)]^3}(C_6 d_4^6 + C_5 d_4^5 + C_4 d_4^4 + C_3 d_4^3 + C_2 d_4^2 + C_1 d_4 + C_0) + O(d_2), \tag{3.30}$$

where

$$C_6 = [\frac{\gamma^2}{d_3^3(1+w_0)^2} - (R_1 - 1)\frac{m}{d_3(1+w_0)^2}]\gamma^5. \tag{3.31}$$

Thus, the sign of Δ_3 is determined by the leading coefficient C_6. In order to have $C_6 < 0$, we can choose appropriate values of γ satisfy $\frac{d_1 d_2 d_3}{1-m} < \gamma < \sqrt{m d_3 (R_1 - 1)}$. Combining the above and theorem 2 in Yu [23], we complete the proof. □

In [8] and [24], it is also proved that infection equilibrium could lose its stability through Hopf bifurcation. Similarly, the conditions given in the above proof (taking small value of d_2 and large value of d_4) are sufficient, but not necessary. There may be many other choices of the parameters that can satisfy this requirement.

4. Numerical illustrations

In this section, we use numerical examples and some simulations to demonstrate the theoretical results obtained in the previous sections. For convenience, we will work on the scaled model (3.16) instead of the original model (2.2). We choose γ as a bifurcation parameter and fix all other parameter values. First, we choose

$$d_1 = 0.001, \quad d_2 = d_5 = 1, \quad d_3 = d_4 = 3, \quad \eta_1 = 3, \quad \eta_2 = 4. \tag{4.1}$$

Then the disease-free equilibrium becomes

$$E_0 = (1000, 0, 0, 0, 0). \tag{4.2}$$

With the parameter values given in (4.1), it's easy to see that $\mathcal{R}_0 = \gamma/0.003$. Note that when $0 < \gamma < 0.003$, $0 < \mathcal{R}_0 < 1$, E_0 is globally asymptotically stable for these given parameter values. Let $\gamma = 1/2000$, the simulation result is shown in Figure 3, indicating that all state variables, except for T, converge to zero, and T converges to 1000. It can be seen that the infected cells first increases and then monotonically decreases rapidly, while T monotonically decreases rapidly and then increases, the other three variables monotonically decrease right from the beginning. They finally reach the disease-free equilibrium E_0.

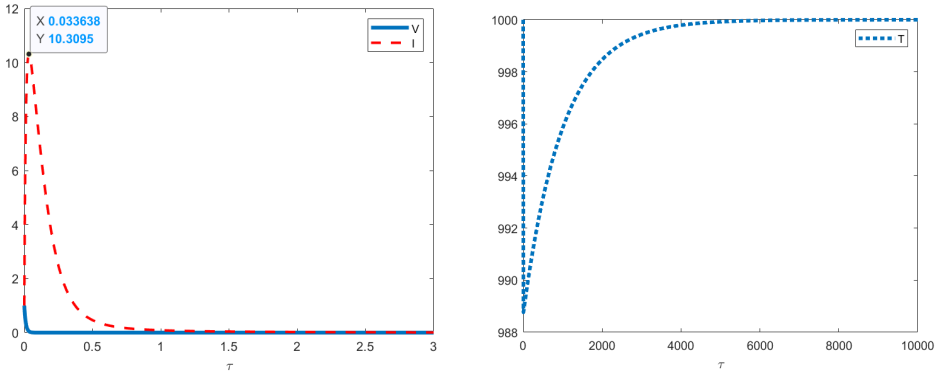

(a) (b)

Figure 3. Simulation of system (3.16) for the parameter values given in (4.1) and $\gamma = \dfrac{1}{2000}$, showing that solution trajectories converge to the disease-free equilibrium E_0.

When γ is increased such that $R_1 < 1$ and $\mathcal{R}_0 > 1$. we choose $\gamma = 1/20$. With the parameter values given in (4.1), the infection equilibrium without defective interfering particles E_1 becomes $(60, 0.94, 0.016, 0, 0)$, which is globally asymptotically stable, as shown in Figure 4. An interesting phenomenon is observed from T, which is no longer monotonically decreasing and then increasing, like the previous case shown in Figure 3, but now it quickly decreases to reach its final steady-state value (see Figure 4). It is also noted that I, V and W converge to their final steady-state values. The equilibrium E_1 in the same time frame (after about 100 days), while I and V reach the E_1 in about 50 days.

When $1 < R_1 < \mathcal{R}_0$, we fix

$$\begin{aligned} &d_1 = 0.001, \quad d_2 = 0.01, \quad d_3 = 3, \quad d_4 = 10, \\ &d_5 = 1, \quad \eta_1 = \frac{100}{3} \quad , \eta_2 = 4. \end{aligned} \tag{4.3}$$

We choose $\gamma = 1/1000$, the infection equilibrium with defective interfering particles E_2 is asymptotically stable. The simulation results are shown in Figure 5. It is seen from this figures that all the state variables now are not monotonically increasing or decreasing, but show oscillating behavior for a quite long period before reaching the equilibrium E_2.

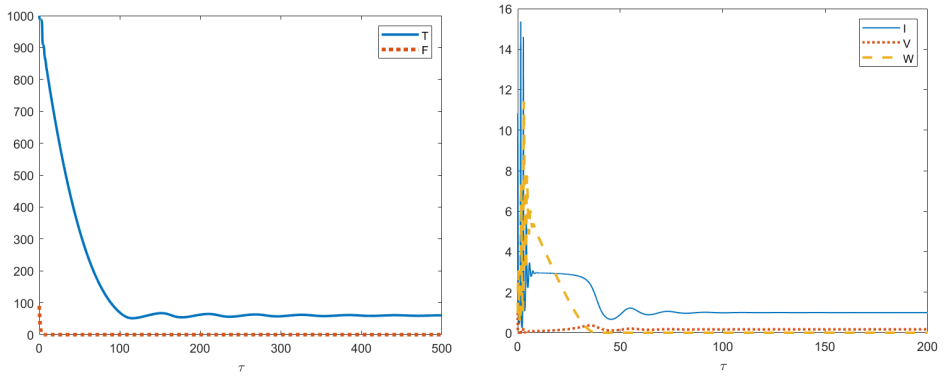

(a) (b)

Figure 4. Simulation of system (3.16) for the parameter values given in (4.1) and $\gamma = 1/20$, showing that solution trajectories converge to the infection equilibrium without defective interefering particles E_1.

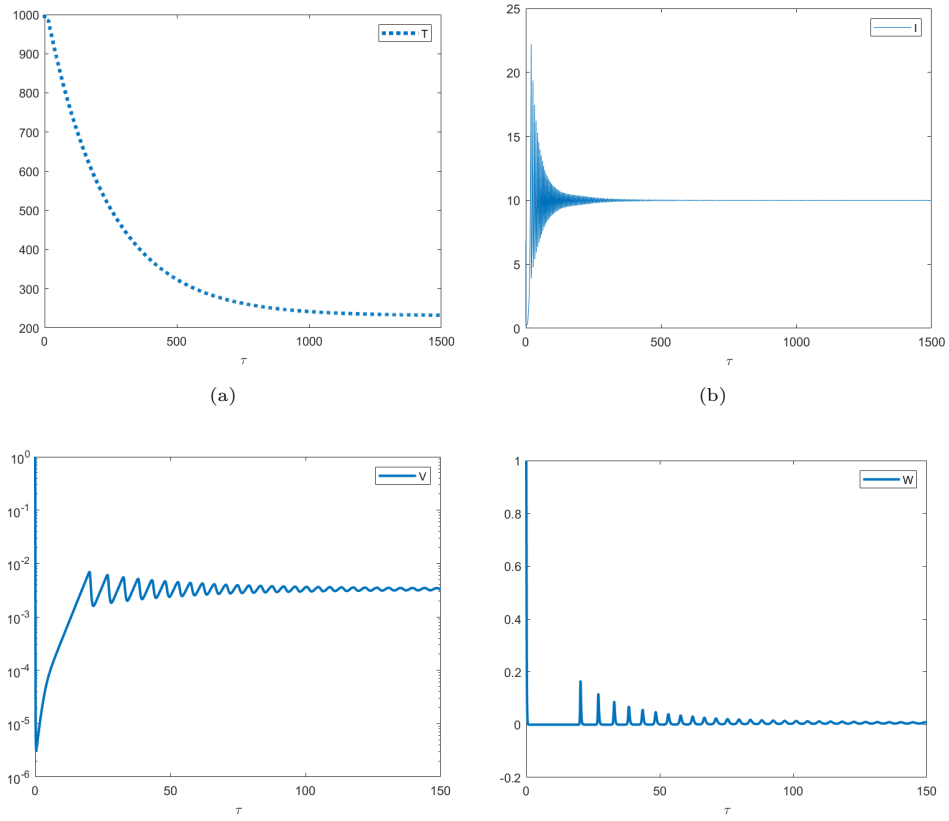

(a) (b)

(c) (d)

Figure 5. Simulation of system (3.16) for the parameter values given in (4.3) and $\gamma = 1/1000$, showing that solution trajectories converge to the infection equilibrium with defective interefering particles E_2.

Finally, we investigate the Hopf bifurcation which occurs from the infectious equilibrium with defective interfering particles E_2. To find the Hopf critical point, we apply the Hurwitz condition in terms of the parameter γ. For the given parameter values, we calculated Δ_3 as follows:

$$\begin{aligned}\Delta_3 =&(810243000000000000000000000000\gamma^6+5401717229160000000000000000000000\gamma^5\\ &+ 900334819877531220000000000000000\gamma^4\\ &+ 10803531688355062440000000000000\gamma^3 + 486151633756162968300000000\gamma^2\\ &+ 97229597531220000000000\gamma + 7292187000000000000)^{-1}\\ &(10800000000000000000000000000000\gamma^9\\ &+ 1285722072900000000000000000000000\gamma^8\\ &- 16983660579758220000000000000000000\gamma^7\\ &- 19422773590223477607940000000000000000\gamma^6\\ &+ 43121973800233504695429242000000000000\gamma^5\\ &- 90826428862874086415187704970000000\gamma^4\\ &-4784257388824726786979089860000\gamma^3-391465897487213335422503474\gamma^2\\ &+ 56845574100039496435020\gamma - 22792256162260830000). \end{aligned} \tag{4.4}$$

A numerical scheme for solving the roots of polynomial can be applied here to find four real solutions of $\Delta_4 = 0$, given by

$$\gamma = 0.0002, \quad -0.0034, \quad 0.0045, \quad -1.1918. \tag{4.5}$$

We choose $\gamma = 0.0002$, the equilibrium solution E_2 becomes unstable and Hopf bifurcation occurs, leading to a family of periodic solutions. The simulation results shown in Figure 6.

5. Conclusion and discussion

In this paper, we proposed a dynamical model for COVID-19 therapy with defective interfering particles and artificial antibodies. We analysed the stability of the disease-free equilibrium E_0, the infection equilibrium without defective interfering particles E_1 and the infection equilibrium with defective interfering particles E_2. When $\mathcal{R}_0 \in (0, 1)$, the E_0 is globally asymptotically stable; when $\mathcal{R}_0 > 1$, $R_1 < 1$, the E_1 is globally asymptotically stable; when $\mathcal{R}_0 \in (R_1, R_2)$, the E_2 is asymptotically stable. When $R_0 > R_2$, the E_2 loses stability and Hopf bifurcation occurs. The E_0 and E_1 exchange their stability at the transcritical point $\mathcal{R}_0 = 1$; and the E_1 and E_2 exchange their stability at the transcritical point $R_1 = 1$; The above descriptions reveal the role that each parameter plays in determining the global dynamics of the model and give some quantitative criteria in terms of the parameters for controlling the infection.

We all know that the basic reproduction number can be used to distinguish whether the disease disappears or not. For equation (3.18), noting that when η_1 decreases, w_0 will increase, and so $\mathcal{R}_0 = \gamma/d_1d_2d_3(1 + w_0)$ will decrease correspondingly. This implies the defective interfering particles do help eliminate the SARS-CoV-2 virus. Since all the parameters in F equation have no impact on the

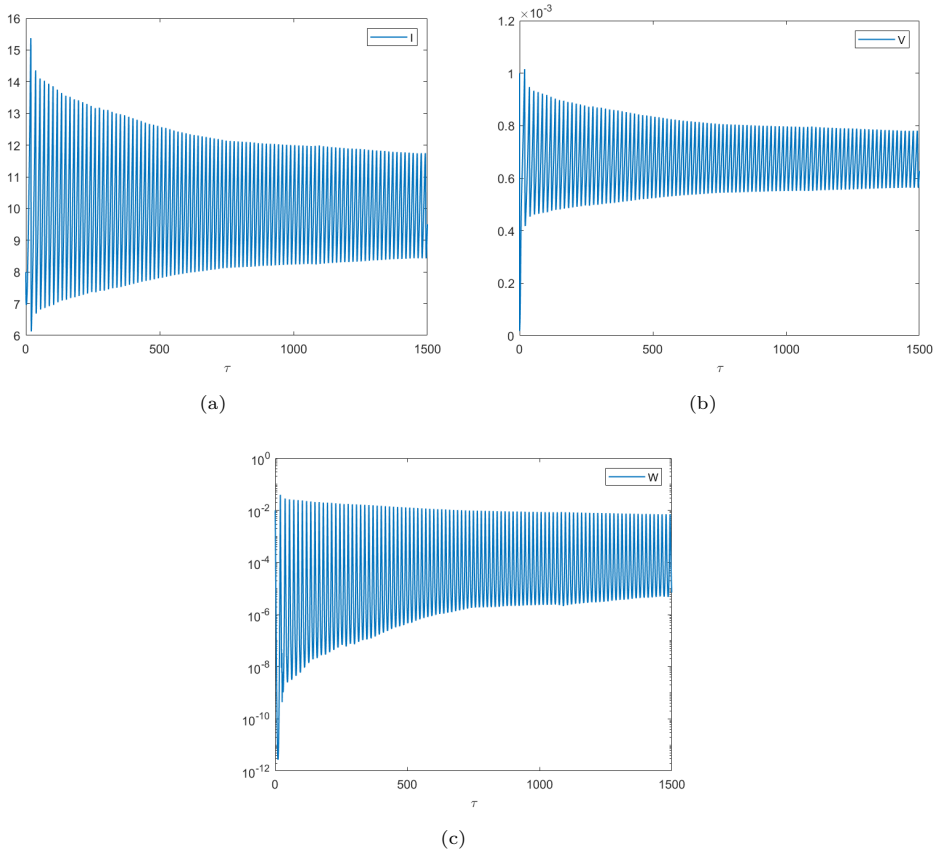

Figure 6. Simulation of system (3.16) for the parameter values given in (4.3) and $\gamma = 0.0002$, showing that periodic solutions.

value of $\mathcal{R}_0$. We conclude that a single time injection of artificial antibodies is not helpful to eliminate the virus completely since artificial antibodies decay to zero throughout the body. We should consider multiple times of injections to ensure that the artificial antibodies persist at a certain level in the body. For example, we assume the injection of artificial antibodies at a constant rate δ, then system (2.2) takes the following form:

$$\begin{aligned}
\frac{dT}{dt} &= \lambda - \alpha TV - d_1 T,\\
\frac{dI}{dt} &= \alpha TV - d_2 I - \eta_1 WI,\\
\frac{dV}{dt} &= \frac{\gamma I}{1+\beta W} - d_3 V - \eta_2 FV,\\
\frac{dW}{dt} &= k\eta_1 WI - d_4 W,\\
\frac{dF}{dt} &= \delta - d_5 F.
\end{aligned} \tag{5.1}$$

Now in terms of the new basic reproduction number $\mathcal{R}_0 = \lambda\alpha\gamma/d_1 d_2(d_3+\eta_2 F_0)(1+w_0)$,

where $F_0 = \delta/d_5$. Obviously, positive δ reduces $\mathcal{R}_0$, implying that both defective interfering particles and artificial antibodies can help eliminate the SARS-CoV-2 virus. This result is of great significance to the elimination of the SARS-CoV-2. At present, antiviral drugs based on this technology have begun preliminary tests and have achieved very gratifying results in animal models [3]. Results of the present study are important not only in relation to therapies against SARS-CoV-2 but also for other diseases for which these biological devices may be developed.

The interaction of virus and cells is a complicated process, which involves cell production, virus attachment to the cells and penetration into the cells, virus replication inside cells and release from cells. Also, the entry of defective interfering particles into the human body will cause more complex reactions, which is not considered in our model.

References

[1] S. F. Ahmed, A. A. Quadeer and M. R. McKay, *Preliminary identification of potential vaccine targets for the COVID-19 coronavirus (SARS-CoV-2) based on SARS-CoV immunological studies*, Viruses, 2020, 12(3), 254.

[2] R. M. Anderson and R. M. May, *Infectious diseases of humans: dynamics and control*, Oxford university press, Oxford, 1992.

[3] P. Chen, A. Nirula, B. Heller et al., *SARS-CoV-2 neutralizing antibody LY-CoV555 in outpatients with COVID-19*, New England Journal of Medicine, 2021, 384(3), 229–237.

[4] P. H. Duesberg, *The RNA of influenza virus*, Proceedings of the National Academy of Sciences of the United States of America, 1968, 59(3), 930.

[5] F. R. Gantmacher and J. L. Brenner, *Applications of the Theory of Matrices*, Courier Corporation, New York, 2005.

[6] L. E. Gralinski and V. D. Menachery, *Return of the coronavirus: 2019-nCoV*, Viruses, 2020, 12(2), 135.

[7] J. J. Holland, S. I. T. Kennedy, B. L. Semler et al., *Defective interfering RNA viruses and the host-cell response*, Springer, 1980. DOI: 10.1007/978-1-4613-3129-2.

[8] X. Jiang, P. Yu, Z. Yuan and X. Zou, *Dynamics of an HIV-1 therapy model of fighting a virus with another virus*, Journal of Biological Dynamics, 2009, 3(4), 387–409.

[9] R. L. Kruse, *Therapeutic strategies in an outbreak scenario to treat the novel coronavirus originating in Wuhan, China*, F1000Research, 2020. DOI: 10-12688/f1000research-22211-2.

[10] J. P. La Salle, *The stability of dynamical systems*, SIAM, Philadelphia, 1976.

[11] Q. Li, X. Guan, P. Wu et al., *Early transmission dynamics in Wuhan, China, of novel coronavirus-infected pneumonia*, New England journal of medicine, 2020. DOI: 10-1056/NEJMoa2001316.

[12] W. Li, M. J. Moore, N. Vasilieva et al., *Angiotensin-converting enzyme 2 is a functional receptor for the SARS coronavirus*, Nature, 2003, 426(6965), 450–454.

[13] P. W. Nelson, J. E. Mittler and A. S. Perelson, *Effect of drug efficacy and the eclipse phase of the viral life cycle on estimates of HIV viral dynamic parameters*, Journal of acquired immune deficiency syndromes (1999), 2001, 26(5), 405–412.

[14] M. Pashaei and N. Rezaei, *Immunotherapy for SARS-CoV-2: potential opportunities*, Expert opinion on biological therapy, 2020, 20(10), 1111–1116.

[15] U. Rand, S. Y. Kupke, H. Shkarlet et al., *Antiviral activity of influenza a virus defective interfering particles against SARS-CoV-2 replication in vitro through stimulation of innate immunity*, bioRxiv, 2021. DOI: 10-1101/2021-02-19-431972.

[16] W. Shang, Y. Yang, Y. Rao and X. Rao, *The outbreak of SARS-CoV-2 pneumonia calls for viral vaccines*, npj Vaccines, 2020, 5(1), 1–3.

[17] Y. Shi, G. Wang, X. Cai et al., *An overview of COVID-19*, Journal of Zhejiang University. Science. B, 2020, 21(5), 343–360.

[18] F. Tapia, T. Laske, M. A. Wasik et al., *Production of defective interfering particles of influenza a virus in parallel continuous cultures at two residence times-insights from QPCR measurements and viral dynamics modeling*, Frontiers in bioengineering and biotechnology, 2019. DOI: 10-3389/fbioe-2019-00275.

[19] M. A. Tortorici and D. Veesler, *Structural insights into coronavirus entry*, Advances in virus research, 2019, 105(4), 93–116.

[20] M. Vignuzzi and C. B. López, *Defective viral genomes are key drivers of the virus-host interaction*, Nature microbiology, 2019, 4(7), 1075–1087.

[21] M. A. Wasik, L. Eichwald, Y. Genzel and U. Reichl, *Cell culture-based production of defective interfering particles for influenza antiviral therapy*, Applied microbiology and biotechnology, 2018, 102(3), 1167–1177.

[22] Y. C. Wu, C. S. Chen and Y. J. Chan, *The outbreak of COVID-19: an overview*, Journal of the Chinese medical association, 2020, 83(3), 217–218.

[23] P. Yu, *Closed-form conditions of bifurcation points for general differential equations*, International Journal of Bifurcation and Chaos, 2005, 15(04), 1467–1483.

[24] P. Yu, J. Huang and J. Jiang, *Dynamics of an HIV-1 infection model with cell mediated immunity*, Communications in Nonlinear Science and Numerical Simulation, 2014, 19(10), 3827–3844.

[25] H. Zhao, K. K. To, H. Chu et al., *Dual-functional peptide with defective interfering genes effectively protects mice against avian and seasonal influenza*, Nature communications, 2018, 9(1), 1–14.